Financial Market Modeling with Quantum Neural Networks*

Carlos Pedro GONÇALVES, Ph. D.
Instituto Superior de Ciências Sociais e Políticas (ISCSP) — University of Lisbon, Portugal
cgoncalves@iscsp.ulisboa.pt

Abstract. Econophysics has developed as a research field that applies the formalism of statistical mechanics and quantum mechanics to address economics and finance problems. The branch of econophysics that applies quantum theory to economics and finance is called quantum econophysics. In finance, quantum econophysics' contributions have ranged from option pricing to market dynamics modeling, behavioral finance and applications of game theory, integrating the empirical finding, from human decision analysis, that shows that nonlinear update rules in probabilities, leading to non-additive decision weights, can be computationally approached from quantum computation, with resulting quantum interference terms explaining the non-additive probabilities. The current work draws on these results to introduce new tools from quantum artificial intelligence, namely quantum artificial neural networks as a way to build and simulate financial market models with adaptive selection of trading rules, leading to turbulence and excess kurtosis in the returns distributions for a wide range of parameters.

Аннотация. Эконофизика сформировалась как исследовательская область, которая применяет понятия статистической механики и квантовой механики для исследования экономических и финансовых проблем. Раздел эконофизики, который применяет квантовую теорию к экономике и финансам, именуется квантовой эконофизикой. В финансовой сфере квантовая эконофизика используется в ряде областей — от оценки опционов до моделирования рыночной динамики. В данной работе вводятся новые инструменты из области квантового искусственного интеллекта, а именно квантовые искусственные нейронные сети в качестве способа создания адаптивных моделей финансовых рынков.

Key words: Finance, econophysics, quantum artificial neural networks, quantum stochastic processes, cognitive science.

1. INTRODUCTION

One of the major problems of financial modeling has been to address complex financial returns dynamics, in particular, excess kurtosis and volatility-related turbulence which lead to statistically significant deviations from the Gaussian random walk model worked in traditional Financial Theory (Arthur *et al.*, 1997; Voit, 2001; Ilinski, 2001; Focardi and Fabozzi, 2004). A main contribution of econophysics to finance has been to address this problem using the tools from statistical mechanics and quantum mechanics, within the paradigmatic basis of systems science and complexity sciences (Anderson *et al.*, 1988; Arthur *et al.*, 1997; Voit, 2001; Ehrentreich, 2008).

Econophysics is currently a major research area that has combined interdisciplinary finance and economics, complex systems science, statistical mechanics, quantum mechanics and cognitive science to address notions and problems in economics and finance (Anderson *et al.*, 1988; Arthur *et al.*, 1997; Voit, 2001; Brunn, 2006; Ehrentreich, 2008; Piotrowski and Sładkowski, 2001, 2002, 2008; Saptsin and Soloviev, 2009, 2011).

There are two major branches in econophysics: classical econophysics (based on classical mechanics) and quantum econophysics (based on quantum mechanics). In finance, quantum econophysics has been applied to option pricing (Segal and Segal, 1998; Baaquie *et al.*, 2000; Baaquie and Marakani, 2001; Baaquie, 2004; Baaquie and Pan, 2011), financial turbulence modeling (Gonçalves, 2011, 2013) and as an approach to the formulation of financial theory, regarding price formation and basic market relations (Piotrowski and Sładkowski, 2001, 2002, 2008; Khrennikov, 2010; Haven and Khrennikov, 2013; Gonçalves, 2011, 2013). Choustova (2007a, b), in particular, argued for the introduction of a quantum-based

* Моделирование финансовых рынков с использованием квантовых нейронных сетей.

approach to financial theory as a way to incorporate market cognition dynamics in financial price formation.

The quantum-based approach goes, however, beyond a good match to price dynamics and turbulence modeling. The growing empirical evidence of quantum interference signatures in human cognition, when faced with decision problems, has led to the development of a quantum theory-based cognitive science forming a theoretical ground for econophysics modeling, with strong implications for finance (Busemeyer and Franco, 2010; Busemeyer and Bruza, 2012; Wang and Busemeyer, 2013; Busemeyer and Wang, 2014; Khrennikov, 2010; Haven and Khrennikov, 2013; Zuo, 2014; Khrennikov and Basieva, 2014).

The main research problem regarding Quantum Theory-based Cognitive Science applied to Finance can be expressed as follows: *if* there is empirical support to the fact that human cognition, in decision problems, leads to a decision behavior computationally isomorphic to quantum adaptive computation (Busemeyer and Franco, 2010; Busemeyer and Bruza, 2012; Wang and Busemeyer, 2013; Busemeyer and Wang, 2014; Zuo, 2014; Khrennikov and Basieva, 2014; Gonçalves, 2015), *then*, the modeling of financial market dynamics needs to work with models of behavior that incorporate, in their probabilistic description, quantum interference terms (Khrennikov, 2010; Haven and Khrennikov, 2013).

This main research problem has led to the growth and development of research lines on cognitive science, working from quantum computer science and quantum information theory, with direct implications for finance and economics, supporting the expansion of quantum econophysics (Khrennikov, 2010; Haven and Khrennikov, 2013), in particular, in regards to finance: opening up the way for research on quantum artificial intelligence (QuAI) applications to financial market modeling (Gonçalves, 2011, 2013).

The current work contributes to such research by introducing Quantum Artificial Neural Networks (QuANNs) for financial market dynamics and volatility risk modeling. In particular, recurrent QuANNs are used to build a model of financial market dynamics that incorporates quantum interference and quantum adaptive computation in the probabilistic description of financial returns. The resulting model shows a quantum-based selection of adaptive rules with consequences for the market dynamics, leading to excess kurtosis and turbulence with clustering volatility, price jumps and statistically significant deviations from Gaussian distributions, for a wide range of parameters.

The work is divided in two parts that are developed in sections 2 and 3. In section 2, the QuANN model is built, simulated and studied, while, in section 3, a reflection is provided on the possible role and contributions of QuAI applied to financial modeling. Regarding the main work, which is developed in section 2, the structure of this section is divided in three subsections.

In subsection 2.1, we review a general framework for classical econophysics modeling of financial market price formation in which Farmer's market making model (Farmer, 2002) is reviewed and combined with multiplicative components, namely: multiplicative volatility components and a market polarization component are introduced in the market making model and linked to trading volume and bullish versus bearish polarization.

In subsection 2.2, we introduce the general formalism of QuANNs, including main notions that form the groundwork for the financial market model. In subsection 2.3, we build the financial market model using a Quantum Neural Automaton (QNA) structure and simulate the resulting artificial financial market, addressing its main results in regards to turbulence and volatility risk, leading to statistically significant deviations from the Gaussian returns distribution.

In section 3, the problem of deviations from the Gaussian random walk is addressed in its relation to econophysics and nonlinear stochastic models of market dynamics, allowing for a reflection on the possible contributions of QuAI and QuANNs for establishing a bridge between the evidence of quantum interference patterns observed in human decision making and a computational basis for nonlinear probability dynamics in finance coming from a linear unitary evolution of networked quantum computation.

2. A QUANN-BASED FINANCIAL MARKET MODEL

2.1 PRICE FORMATION AND FINANCIAL RETURNS

Following Farmer (2002) and Ilinski (2001), financial market price formation can be linked to unbalanced market orders M, where $M > 0$ corresponds to an excess demand while $M < 0$ to an excess supply, such that, for a financial risky asset, traded at discrete trading rounds of duration Δt, the asset price at t, $S(t)$ depends upon the previous price $S(t-\Delta t)$ and the market orders that arrive during the trading round. A few basic assumptions, in classical econophysics, determine the structure for the relation between market orders and the new price (Farmer, 2002; Ilinski, 2001):

The price is assumed as a finite increasing function of the previous price and order size $M(t)$:

$$S(t) = f_S\left(S(t-\Delta t), M(t)\right) \qquad (1)$$

If the order size is null $M(t) = 0$ the market clears for equal supply and demand, so that there is no market impact (the price stays unchanged):

$$f_S\left(S(t-\Delta t),0\right) = S(t-\Delta t) \quad (2)$$

There are no arbitrage opportunities associated with a sequence of trades that sum zero (a repeated trading through a circuit);

Gauge invariance with respect to currency units, so that the only possible combination for prices to enter is $S(t)/\mathrm{S}(t-\Delta t)$, such that:

$$\frac{S(t)}{S(t-\Delta t)} = \frac{f_S\left(S(t-\Delta t), M(t)\right)}{S(t-\Delta t)} = F\left(M(t)\right) \quad (3)$$

The result of these four assumptions is the general form for F in Eq. (3) given by (Farmer, 2002; Ilinski, 2001):

$$F\left(M(t)\right) = e^{\frac{M(t)}{\lambda}} \quad (4)$$

where λ is a liquidity parameter, also called market depth (Farmer, 2002). The result from Eq. (4), replaced in Eq. (3) is the following dynamical rule:

$$S(t) = S(t-\Delta t)e^{\frac{M(t)}{\lambda}} \quad (5)$$

or, taking the logarithms, the log-price rule (Farmer, 2002; Ilinski, 2001):

$$\ln S(t) = \ln S(t-\Delta t) + \frac{M(t)}{\lambda} \quad (6)$$

There are two dynamical components to $M(t)$: the sign, which can either be positive (excess of buy orders) or negative (excess of sell orders), and the volume of unbalanced market orders, which is linked to the order size.

Within financial theory, the order size can be worked from a systemic market dynamics that leads to the formation of consensus clusters regarding the decision to invest greater or smaller amounts, or, alternatively, to sell greater or smaller amounts.

The adaptive management of exposure to asset price fluctuation risk, on the part of market agents, given information that impacts asset value leads to a two-sided aspect of computation of financial information by the market system: on the one hand, there is the matter whether each new information is good (*bullish*) or bad (*bearish*), in terms of asset value, on the other hand, there is the degree to which new information supports the decision to buy or sell by different amounts (the market volume aspect).

A social consensus dynamics coming from market computation can be linked to consensus clusters affecting the market unbalance, so that the positive or negative sign can be addressed, within econophysics, in terms of a notion of spin. In physics the spin is a fundamental degree of freedom of field quanta that behaves like angular momentum, the spin quantum numbers assume integer and half-integer values, the most elementary case of half integer spin is the spin-1/2.

Considering a three dimensional axes system, if a spin-1/2 particle's spin state is measured along the z-axis then there are two fundamental orientations *spin up* and *spin down*, in complex systems science these two orientations are assumed and worked mainly from the statistical mechanics of Ising systems as models of complex systems (Kauffman, 1993), which constituted early inspiration for econophysics' models of financial markets (Vaga, 1990; Iiori, 1999; Lux and Marchesi, 1999; Voit, 2001). These models allowed for the study of polarization in market sentiment, working with the statistical mechanics of Ising systems, allowing direct connections to cognitive science (Voit, 2001).

The market volume, on the other hand, has been addressed, within financial theory, by multiplicative processes (Mandelbrot, *et al.*, 1997; Mandelbrot, 1997), drawing upon Mandelbrot's work on turbulence in statistical mechanics, as reviewed in Mandelbrot (1997). The multiplicative stochastic processes, worked by Mandelbrot and connected to multifractal geometry, led to Mandelbrot *et al.* 's (1997) Multifractal Model of Asset Returns (MMAR), which also inspired modified versions using multiplicative stochastic processes with Markov switching in volatility components (Calvet and Fisher, 2004; Lux, 2008).

Considering Eq. (6), a spin-1/2 like model can be integrated as a binary component in a multiplicative model that includes market volume, by way of a multiplicative decomposition of $M(t)$ in a market polarization component $\sigma(t) = \pm 1$, and N trading volume-related volatility components, so that we obtain:

$$M(t) = \left(\prod_{k=1}^{N} V_k(t)\right)\sigma(t) \quad (7)$$

where each volatility component $V_k(t)$ can assume one of two values v_0 or $v_1 = 2 - v_0$. If $0 < v_0 \leq 1$, then v_0 corresponds to a low volatility state, while v_1 to a high volatility state (v_0 diminishes the returns' value while v_1 amplifies the returns value like a lever). The logarithmic returns for the risky asset, in this approach, are given by:

$$R(t) = \ln \frac{S(t)}{S(t-\Delta t)} = \frac{1}{\lambda}\left(\prod_{k=1}^{N} V_k(t)\right)\sigma(t) \qquad (8)$$

The binary structure assumed for the N components plus the market polarization, makes this model a good starting point for QuANN applications, since QuANNs also work from a binary computational basis to address neural firing patterns.

On the other hand, QuANNs open up the possibility for dealing with the multiplicative models in such a way that the probabilities, rather than being introduced from a top-down ex-ante fixed state-transition probability distribution, change from trading round to trading round, being the result of the quantum computational process introduced for each returns' component.

QuANNs also allow one to incorporate the empirical evidence that human cognition, when addressing decision between alternatives, follows a dynamics that is computationally isomorphic to quantum computation applied to decision science, leading to interference effects with an expression in decision frequencies (probabilities), which means that, when considering probabilities for human behavior, the theoretical framework of networked quantum computation may be more appropriate for the dynamical modeling of human systems.

In the quantum description, Eq. (8) will be expressed in operator form on an appropriate Hilbert space, with the returns operator's eigenvalues being addressed from the QuANN structure, which works with *quantum bits* (*qubits*), whose computational basis states describe the neuron's firing pattern in terms of firing (ON) and non-firing (OFF)[1]. In order to build the market model, however, we need to introduce, first, a general framework for QuANNs which will then be applied to the risky asset price dynamics modeling.

2.2 QUANTUM ARTIFICIAL NEURAL NETWORKS

The connection between quantum computer science and ANNs has been object of research since the 1990s, in particular, in what regards quantum associative memory, quantum parallel processing, extension of classical ANN schemes, as well as computational complexity and efficiency of QuANNs over classical ANNs (Chrisley, 1995; Kak, 1995; Menneer and Narayanan, 1995; Behrman *et al.*, 1996; Menneer, 1998; Ivancevic and Ivancevic, 2010; Gonçalves, 2015).

Mathematically, a classical ANN with a binary firing pattern can be defined as an artificial networked computing system comprised of a directed graph (digraph) with the following additional structure (McCulloch and Pitts, 1943; Müller *et al.*, 1995):

- A binary alphabet $A_2 = \{0,1\}$ associated to each neuron describing the neural activity, with 0 corresponding to a non-firing neural state and 1 to a firing neural state, so that the firing patterns of a neural network with N neurons are expressed by the set of all binary strings of length N: $A_2^N = \{s_1 s_2 ... s_N : s_k \in A_2, k = 1,2,...,N\}$;
- A real-valued weight associated with each neural link, expressing the strength and type of neural connection;
- A transfer function which determines the state transition of the neuron and that depends upon: the state of its incident neurons, the weight associated with each incoming neural links and an activation threshold that can be specific for each neuron.

A quantum version of ANNs, on the other hand, can be defined as a directed graph with a networked quantum computing structure, such that (Gonçalves, 2015):

- To each neuron is associated a two-dimensional Hilbert Space H_2 spanned by the computational basis $B_2 = \{|0\rangle, |1\rangle\}$, where $|0\rangle, |1\rangle$ are ket vectors (in Dirac's *bra-ket* notation for Quantum Mechanics' vector-based formalism using Hilbert spaces[2]), where $|0\rangle$ encodes a non-firing neural dynamics and $|1\rangle$ encodes a firing neural dynamics;
- To a neural network, comprised of N neurons, is associated the tensor product of N copies of H_2, so that the neural network's Hilbert space is the space $H_2^{\otimes N}$ spanned by the basis $B_2^{\otimes N} = \{|\mathbf{s}\rangle : \mathbf{s} \in A_2^N\}$ which encodes all the alternative firing patterns of the neurons;
- The general neural configuration state of the neural network is characterized by a normalized ket vector $|\psi\rangle \in H_2^{\otimes N}$ expanded in the neural firing patterns' basis $B_2^{\otimes N}$:

$$|\psi\rangle = \sum_{\mathbf{s} \in A_2^N} \psi(\mathbf{s}) |\mathbf{s}\rangle \qquad (9)$$

with the normalization condition:

$$\sum_{\mathbf{s} \in A_2^N} |\psi(\mathbf{s})|^2 = 1 \qquad (10)$$

[1] This degree of freedom behaves like spin, so that the neuron's associated qubit can also be approached in terms of a spin-1/2 model.

[2] We use the vector representation convention introduced by Dirac (1967) for Hilbert spaces, assumed and used extensively in Quantum Mechanics. In this case, a *ket vector*, represented as $|a\rangle$, is a column vector of complex numbers while a *bra vector*, represented as $\langle a|$, is the conjugate transpose of $|a\rangle$, that is: $\langle a| = |a\rangle^{\dagger}$. The Hilbert space inner product is represented as $(|a\rangle, |b\rangle) = \langle a|b\rangle$. The outer product is, in turn, given by $|a\rangle\langle b|$. A projection operator corresponds to an operator of the form $\hat{P}_a = |a\rangle\langle a|$ which acts on any ket $|b\rangle$ as $\hat{P}_a|b\rangle = \langle a|b\rangle|a\rangle$.

The neural network has an associated neural links state transition operator $\hat{L}_{Net}$ such that, given an input neural state $|\psi_{in}\rangle$, the operator transforms the input state for the neural network in an output state $|\psi_{out}\rangle$, reflecting, in this operation, the neural links for the neural network, so that each neuron has an associated structure of unitary operators that is conditional on its input neurons:

$$|\psi_{out}\rangle = \hat{L}_{Net}|\psi_{in}\rangle \quad (11)$$

The output state of a QuANN shows, in general, complex quantum correlations so that the quantum dynamics of a single neuron may depend in a complex way on the entire neural network's configuration (Gonçalves, 2015). Considering the neurons n_1, ..., n_N for a N-neuron neural network, the $\hat{L}_{Net}$ operator can be expressed as a product of each neuron's neural links operator following the ordered sequence $n_1, ..., n_N$, where neuron n_1 is the first to be updated and n_N the last (that is, following the activation sequence[3]):

$$\hat{L}_{Net} = \hat{L}_N ... \hat{L}_2 \hat{L}_1 \quad (12)$$

Each neuron's neural links operator is a quantum generalization of an activation function, with the following structure for the k-th neuron:

$$\hat{L}_k = \sum_{\mathbf{s}\in A_2^{k-1}, \mathbf{s}'\in A_2^{N-k}} |\mathbf{s}\rangle\langle\mathbf{s}| \otimes L_k(\mathbf{s}_{in}) \otimes |\mathbf{s}'\rangle\langle\mathbf{s}'| \quad (13)$$

where $\mathbf{s}_{in}$ is a substring, taken from the binary word **ss′**, that matches in **ss′** the activation pattern for the input neurons of n_k, under the neural network's architecture, in the same order and binary sequence as it appears in **ss′**, $L_k(\mathbf{s}_{in})$ is a neural links function that maps the input substring to a unitary operator on the two-dimensional Hilbert space H_2, this means that, for different configurations of the neural network, the neural links operator for the k-th neuron $\hat{L}_k$ assigns a corresponding unitary operator that depends upon the activation pattern of the input neurons.

The neural links operators incorporate the local structure of neural connections so that there is a unitary state transition for the neuron (a quantum computation) conditional upon the firing pattern of its input neurons.

[3] For some QuANNs it is possible to consider the action of the operators conjointly and to introduce, in one single neural links operator, a transformation of multiple neurons' states, taking advantage of parallel quantum computation (Gonçalves, 2015).

Now, an arbitrary unitary operator on a single-*qubit* Hilbert space H_2 is a member of the unitary group U (2) and can be derived from a specific Hamiltonian operator structure (Greiner and Müller, 2001), so that we have, for a QuANN, a conditional unitary state transition:

$$L_k(\mathbf{s}_{in}) = e^{-\frac{i}{\hbar}\Delta t \hat{H}_{\mathbf{s}_{in}}} \quad (14)$$

where the neuron's associated Hamiltonian operator $\hat{H}_{\mathbf{s}_{in}}$ is conditional on the input neurons' firing pattern $\mathbf{s}_{in}$ and given by the general structure:

$$\hat{H}_{\mathbf{s}_{in}} = -\frac{\omega(\mathbf{s}_{in})}{2}\hbar\hat{1} + \theta(\mathbf{s}_{in})\sum_{j=1}^{3} u_j(\mathbf{s}_{in})\frac{\hbar}{2}\hat{\sigma}_j \quad (15)$$

where ħ is the reduced Planck constant[4], $\theta(\mathbf{s}_{in})$, $\omega(\mathbf{s}_{in})$ are measured in radians per second and depend upon the neural configuration for the input neurons, $\hat{1}$ is the unit operator on H_2, the $u_j(\mathbf{s}_{in})$ terms are the components of a real unit vector $\mathbf{u}(\mathbf{s}_{in})$ and $\hat{\sigma}_j$ are Pauli's operators[5]:

$$\hat{\sigma}_1 = |0\rangle\langle 1| + |1\rangle\langle 0| = \begin{pmatrix} 0 & 1 \\ 1 & 0 \end{pmatrix} \quad (16)$$

$$\hat{\sigma}_2 = -i|0\rangle\langle 1| + i|1\rangle\langle 0| = \begin{pmatrix} 0 & -i \\ i & 0 \end{pmatrix} \quad (17)$$

$$\hat{\sigma}_3 = |0\rangle\langle 0| - |1\rangle\langle 1| = \begin{pmatrix} 1 & 0 \\ 0 & -1 \end{pmatrix} \quad (18)$$

Replacing Eq. (15) in Eq. (14) and expanding we obtain:

$$L_k(\mathbf{s}_{in}) = e^{-\frac{i}{\hbar}\Delta t \hat{H}_{\mathbf{s}_{in}}} = e^{i\frac{\omega(\mathbf{s}_{in})\Delta t}{2}} \begin{bmatrix} \cos\left(\frac{\theta(\mathbf{s}_{in})\Delta t}{2}\right)\hat{1} - \\ -i\sin\left(\frac{\theta(\mathbf{s}_{in})\Delta t}{2}\right)\sum_{j=1}^{3} u_j(\mathbf{s}_{in})\hat{\sigma}_j \end{bmatrix} \quad (19)$$

The operator in Eq. (19) is comprised of the product of a phase transformation ($i\omega(\mathbf{s}_{in})\Delta t/2$) and a rotation operator defined as (Greiner and Müller, 2001; Nielsen and Chuang, 2003):

[4] $1.054571800(13)\times10^{-34}$ Js

[5] The terms $(\hbar/2)\hat{\sigma}_j$, in the Hamiltonian, are equivalent to the spin operators for a spin-1/2 system (Leggett, 2002).

$$\hat{R}_{\mathbf{u}(\mathbf{s}_{in})}\left[\theta(\mathbf{s}_{in}),\Delta t\right]=\cos\left(\frac{\theta(\mathbf{s}_{in})\Delta t}{2}\right)\hat{1}-i\sin\left(\frac{\theta(\mathbf{s}_{in})\Delta t}{2}\right)\sum_{j=1}^{3}u_{j}(\mathbf{s}_{in})\hat{\sigma}_{j} \tag{20}$$

An arbitrary single-*qubit* unitary operator (a quantum logic gate on a *qubit*) can, thus, be expressed by the product (Nielsen and Chuang, 2003):

$$e^{-\frac{i}{\hbar}\hat{H}_{\mathbf{s}_{in}}\Delta t}=\exp\left(i\frac{\omega(\mathbf{s}_{in})\Delta t}{2}\right)\hat{R}_{\mathbf{u}(\mathbf{s}_{in})}\left[\theta(\mathbf{s}_{in})\Delta t\right] \tag{21}$$

This means that the transfer function of classical ANNs is replaced, for QuANNs, by phase transformations and rotations of the neuron's quantum state conditional upon the firing pattern of the input neurons[6].

Now, given an operator $\hat{O}$ on the neural network's Hilbert space $\mathrm{H}_{2}^{\otimes N}$ expanded as:

$$\hat{O}=\sum_{\mathbf{s},\mathbf{s}'\in\mathrm{A}_{2}^{N}}O_{\mathbf{s},\mathbf{s}'}\left|\mathbf{s}\right\rangle\left\langle\mathbf{s}'\right| \tag{22}$$

taking the inner product between a normalized ket vector $\left|\psi\right\rangle$ and the transformed vector $\hat{O}\left|\psi\right\rangle$ yields:

$$\left(\left|\psi\right\rangle,\hat{O}\left|\psi\right\rangle\right)=\left\langle\psi\left|\hat{O}\right|\psi\right\rangle=\sum_{\mathbf{s},\mathbf{s}'\in\mathrm{A}_{2}^{N}}O_{\mathbf{s},\mathbf{s}'}\left\langle\mathbf{s}'\mid\psi\right\rangle\left\langle\psi\mid\mathbf{s}\right\rangle=\sum_{\mathbf{s},\mathbf{s}'\in\mathrm{A}_{2}^{N}}O_{\mathbf{s},\mathbf{s}'}\psi(\mathbf{s}')\psi(\mathbf{s})^{*} \tag{23}$$

For Hermitian operators obeying the relation:

$$O_{\mathbf{s},\mathbf{s}'}\left\langle\mathbf{s}'\mid\psi\right\rangle\left\langle\psi\mid\mathbf{s}\right\rangle\delta_{\mathbf{s},\mathbf{s}'} \tag{24}$$

given that the state vector is normalized, if this relation is verified, then Eq. (23) yields a classical expectation in which the amplitudes in square modulus $|\psi(\mathbf{s})|^{2}$ are equivalent to decision weights associated with each alternative value on the diagonal of the operator's matrix representation:

$$\left\langle\hat{O}\right\rangle_{\psi}=\left\langle\psi\left|\hat{O}\right|\psi\right\rangle=\sum_{\mathbf{s}\in\mathrm{A}_{2}^{N}}O_{\mathbf{s},\mathbf{s}}\mid\psi(\mathbf{s})\mid^{2} \tag{25}$$

so that, for a neural network in the state $\left|\psi\right\rangle$, the neural activity can be described by the value $O_{\mathbf{s},\mathbf{s}}$ with an associated weight of $|\psi(\mathbf{s})|^{2}$.

In the case of econophysics, as well as game theory applications, one usually assumes that the social system tends to the alternatives in proportion to the corresponding decision weights, such that one can associate a probability measure for the system to follow each alternative as numerically coincident to the corresponding decision weight. This is akin to game theory's notion of mixed strategy, in the sense that each player can be characterized by a fixed mixed strategy and play probabilistically according to the mixed strategy's weights.

While the probability of a player's behavior is zero or one after play, the decision weights remain the same, in the case of game theory this means that the Nash equilibrium does not change, being available as a cognitive strategic scheme for further plays (Nash, 1951). In applications of QuANNs to social systems this means that one needs to work with either an Everettian interpretation of quantum theory, or with a Bohmian interpretation[7].

The Bohmian interpretation is often assumed by researchers dealing with econophysics (Choustova, 2007a, b; Khrennikov, 2010; Haven and Khrennikov, 2013), in particular, when one wishes to address the amplitudes in square modulus $|\psi(\mathbf{s})|^{2}$ in terms of economic forces linked to emergent degrees of freedom that tend to make the system follow certain paths probabilistically (a quantum-based probabilistic version of Haken's slaving principle applied to economic and financial systems (Haken, 1977)).

The Everettian line of interpretations has, since its initial proposal by Everett (1957, 1973), been directly linked to a Cybernetics' paradigmatic basis incorporating both automata theory and information theory

[6] This leads to quantum correlations that reflect the neural network's structure (Gonçalves, 2015).

[7] Since these are the two lines of interpretation that do not assume a state vector collapse.

(Gonçalves, 2015), a point that comes directly from Everett's original work on quantum mechanics, that is further deepened by Deutsch's work on quantum computation (Deutsch, 1985), and, later, on quantum decision theory (Deutsch, 1999; Wallace, 2002, 2007).

There are actually different perspectives from different authors on Everett's original proposal (Bruce, 2004). Formally, the proposal is close to Bohm's, including the importance attributed to computation and to information theory, however, systemically, Bohm and Everett are very distinct in the hypotheses they raise: for Bohm the state vector is assumed to represent a statistical average of an underlying information field's sub-quantum dynamics (Bohm, 1984; Bohm and Hiley, 1993), Everett (1957, 1973) assumes the geometry of the Hilbert space as the correct description of the fundamental dynamics of fields and systems.

Considering QuANNs, under Everett's approach, we can introduce the set of projection operators onto the basis $\mathrm{B}_2^{\otimes N}$, $\mathrm{P}=\left\{\hat{P}_{\mathbf{s}}=|\mathbf{s}\rangle\langle\mathbf{s}|:\mathbf{s}\in \mathrm{A}_2^N\right\}$ where each operator has the matrix representation $P_{\mathbf{s},\mathbf{s}'}=\delta_{\mathbf{s},\mathbf{s}'}$, these operators form a complete set of orthogonal projectors, since their sum equals the unit operator on the Hilbert space $\mathrm{H}_2^{\otimes N}$, $\sum_{\mathbf{s}\in \mathrm{A}_2^N}\hat{P}_{\mathbf{s}}=\hat{1}^{\otimes N}$, and they are mutually exclusive, that is, the product of two of these operators obeys the relation $\delta_{\mathbf{s},\mathbf{s}'}\hat{P}_{\mathbf{s}}\hat{P}_{\mathbf{s}'}$.

A projection operator can represent a projective computation, by the neural network, of an alternative neural firing pattern for the network. The general state vector in Eq. (9) can, thus, be expressed as a sum of projections, that is, the neural network's quantum state has a projective expression over each alternative neural configuration simultaneously, corresponding to a simultaneous systemic projective activity over all alternatives:

$$|\psi\rangle=\sum_{\mathbf{s}\in \mathrm{A}_2^N}\hat{P}_{\mathbf{s}}|\psi\rangle \tag{26}$$

Each alternative neural configuration corresponds to an orthogonal dimension of the 2^N dimensional Hilbert space $\mathrm{H}_2^{\otimes N}$, a dimension that is spanned by a corresponding basis vector in $\mathrm{B}_2^{\otimes N}$, which means that the quantum system (in our case, the QuANN) projects simultaneously over each (orthogonal) dimension of systemic activity (corresponding, in our case, to each alternative neural pattern) weighing each dimension. The weight of the projection over a given dimension (a given pattern of systemic activity) in the system's state can be worked from a notion of norm. Using the Hilbert space's inner product structure, we can work with the squared norm of the projected vector, which leads to:

$$\begin{aligned}\left\|\hat{P}_{\mathbf{s}}|\psi\rangle\right\|^2&=(\hat{P}_{\mathbf{s}}|\psi\rangle,\hat{P}_{\mathbf{s}}|\psi\rangle)=\\&=\left\langle\psi\left|\hat{P}_{\mathbf{s}}^{\dagger}\hat{P}_{\mathbf{s}}\right|\psi\right\rangle=|\psi(\mathbf{s})|^2\end{aligned} \tag{27}$$

Systemically, this last equation can be interpreted as expressing that the weight of the projection $\hat{P}_{\mathbf{s}}$, in the system's projective dynamics, is equal to $|\psi(\mathbf{s})|^2$. In this sense, each orthogonal dimension corresponds to a distinct pattern of activity that is projectively computed by the system.

On the other hand, for a large ensemble of QuANNs with the same structure and in the same state, the statistical weight associated to the projection operator $\hat{P}_{\mathbf{s}}$, expressed by the ensemble average $\left\langle\hat{P}_{\mathbf{s}}\right\rangle$, coincides with the projection weight $|\psi(\mathbf{s})|^2$ associated to the neural state projection $\hat{P}_{\mathbf{s}}|\psi\rangle$, thus, the statistical interpretation comes directly from the projective structure of the state vector. Indeed, let us consider a statistical ensemble of M QuANNs such that each QuANN has the same number of neurons N and the same architecture, let us, further, assume that each neural network is characterized by some quantum neural state $|\psi_k\rangle$, with $k=1,2,\ldots,M$, the ensemble state can be represented by a statistical density operator:

$$\hat{\rho}=\frac{1}{M}\sum_{k=1}^{M}|\psi_k\rangle\langle\psi_k| \tag{28}$$

The statistical average of an operator $\hat{O}$ on the Hilbert space $\mathrm{H}_2^{\otimes N}$ is given by (Bransden and Joachain, 2000):

$$\begin{aligned}\left\langle\hat{O}\right\rangle&=Tr(\hat{O}\hat{\rho})=\\&=\frac{1}{M}\sum_{k=1}^{M}\sum_{\mathbf{s},\mathbf{s}'\in \mathrm{A}_2^N}O_{\mathbf{s},\mathbf{s}'}\langle\mathbf{s}'|\psi_k\rangle\langle\psi_k|\mathbf{s}\rangle\\&=\frac{1}{M}\sum_{k=1}^{M}\left\langle\psi_k\left|\hat{O}\right|\psi_k\right\rangle=\frac{1}{M}\sum_{k=1}^{M}\left\langle\hat{O}\right\rangle_{\psi_k}\end{aligned} \tag{29}$$

for a projector on the neural basis we get the ensemble average:

$$\left\langle\hat{P}_{\mathbf{s}}\right\rangle=\frac{1}{M}\sum_{k=1}^{M}\left\langle\psi_k\left|\hat{P}_{\mathbf{s}}\right|\psi_k\right\rangle=\frac{1}{M}\sum_{k=1}^{M}|\psi_k(\mathbf{s})|^2 \tag{30}$$

Now, if all the members of the ensemble are in the same neural state $|\psi_k\rangle=|\psi\rangle$ for each $k=1,\ldots,M$ the whole statistical weight that is placed on the projection coincides exactly with $|\psi(\mathbf{s})|^2$ so that the ensemble average of the projection coincides numerically with the degree to which the system projects over the dimension corresponding to the neural pattern $|\mathbf{s}\rangle$

(the projection norm), that is, there is a numerical coincidence between $\left\|\hat{P}_{\mathbf{s}}\left|\psi\right\rangle\right\|^2$ and $\left\langle\hat{P}_{\mathbf{s}}\right\rangle$:

$$\left\langle\hat{P}_{\mathbf{s}}\right\rangle=\frac{1}{M}\sum_{k=1}^{M}\left|\psi(\mathbf{s})\right|^2=\left|\psi(\mathbf{s})\right|^2 \tag{31}$$

Thus, an ensemble of QuANNs with the same structure, characterized by the same quantum state $\left|\psi\right\rangle$, has a statistical weight for each projection coincident with the norm of the projection, so that this norm has a statistical expression once we consider an ensemble of systems with the same structure and characterized by the same state.

This is similar to the argument that is made around repeated independent[8] and identically prepared experiments leading to a statistical distribution that shows the markers of the underlying quantum dynamics, in that case, we also see a statistical ensemble marker (considering an ensemble of experiments with the same state vector) that recovers the projection norm structure in the statistical distribution.

The experiments, in the case of human systems, have led to the finding of the same computational properties and projective dynamics present in the quantum systems (Busemeyer and Franco, 2010; Busemeyer and Bruza, 2012; Wang and Busemeyer, 2013; Busemeyer and Wang, 2014), a finding that comes from the statistical distribution of the experiments.

In an econophysics setting, the projective dynamics can be addressed as a cognitive projection such that the projection norm corresponds to the decision weight placed on that alternative[9]. The QuANN state transition has an implication in the projection weights, in the sense that given the state transition:

$$\left|\psi_{out}\right\rangle=\hat{L}_{Net}\left|\psi_{in}\right\rangle=\sum_{\mathbf{s}\in A_2^N}\psi_{out}(\mathbf{s})\left|\mathbf{s}\right\rangle, \tag{32}$$

the output amplitudes are given by:

$$\begin{aligned}\psi_{out}(\mathbf{s})&=\sum_{\mathbf{s}'\in A_2^N}\left\langle\mathbf{s}\left|\hat{L}_{Net}\right|\mathbf{s}'\right\rangle\left\langle\mathbf{s}'\mid\psi_{in}\right\rangle=\\&=\sum_{\mathbf{s}'\in A_2^N}L_{Net}(\mathbf{s},\mathbf{s}')\psi_{in}(\mathbf{s}')\end{aligned} \tag{33}$$

with $L_{Net}(\mathbf{s},\mathbf{s}')=\left\langle\mathbf{s}\left|\hat{L}_{Net}\right|\mathbf{s}'\right\rangle$. Eq. (33) means that the following change in the projections' norms takes place:

$$\begin{aligned}&\left\|\hat{P}_{\mathbf{s}}\left|\psi_{in}\right\rangle\right\|^2=|\,\psi_{in}(\mathbf{s})\,|^2\rightarrow\\&\rightarrow\left\|\hat{P}_{\mathbf{s}}\left|\psi_{out}\right\rangle\right\|^2=|\,\psi_{out}(\mathbf{s})\,|^2=\left|\sum_{\mathbf{s}'\in A_2^N}L_{Net}(\mathbf{s},\mathbf{s}')\psi_{in}(\mathbf{s}')\right|^2\end{aligned} \tag{34}$$

The sum within the square modulus is a source of quantum interference at the projection norm level.

An iterative scheme with the repeated application of the neural network operator $\hat{L}_{Net}$ leads to a sequence of quantum neural states $\left|\psi(t)\right\rangle$. Expanding the complex numbers associated to the quantum amplitudes:

$$\left\langle\mathbf{s}\mid\psi(t)\right\rangle=\psi(\mathbf{s},t)=\sqrt{A(\mathbf{s},t)}+i\sqrt{B(\mathbf{s},t)} \tag{35}$$

We can express the dynamical variables $A(\mathbf{s}, t)$ and $B(\mathbf{s}, t)$ in terms of a dynamical nonlinear state transition rule:

$$A(\mathbf{s},t)=\left[Re\left(\sum_{\mathbf{s}'\in A_2^N}L_{Net}(\mathbf{s},\mathbf{s}')\psi(\mathbf{s}',t-\Delta t)\right)\right]^2 \tag{36}$$

$$B(\mathbf{s},t)=\left[Im\left(\sum_{\mathbf{s}'\in A_2^N}L_{Net}(\mathbf{s},\mathbf{s}')\psi(\mathbf{s}',t-\Delta t)\right)\right]^2 \tag{37}$$

which leads to a 2^{N+1} system of nonlinear equations, from where it follows that the probability associated to a given neural firing configuration, worked from the expected projection (in accordance with the ensemble average), is given by the sum of the two dynamical variables:

$$Prob[\mathbf{s},t]=A(\mathbf{s},t)+B(\mathbf{s},t) \tag{38}$$

[8] In the case of QuANNs this presupposes the non-interaction between the ensemble elements, appealing to a description of a statistical random sample.

[9] In the quantum computational setting, under the Everettian line, the projective structure for QuANNs can be considered as a computational projection such that each Hilbert space dimension, corresponding to a different neural pattern, is computed simultaneously with an associated weight (given by the norm of the projection), having a computational expression in the system's quantum processing and a statistical correspondence in the neural activity pattern of an ensemble of QuANNs with the same structure and in the same state (assuming non-interaction between different ensemble elements). In the case of physical systems, the projective dynamics, interpreted computationally, leads to a physical expression of the system at multiple dimensions of systemic activity, a point which was interpreted by DeWitt (1970) under the notion of many worlds of a same universe, where each world corresponds to an entire configuration of the universe matching a corresponding orthogonal dimension of an appropriate Hilbert space where observers and systems are correlated (entanglement). In the case of applications to human decision-making, the orthogonal dimensions can be assumed to correspond to alternative decision scenarios evaluated by the decision-maker and supporting his/her choice.

This establishes a bridge between Nonlinear Dynamical Systems Theory and quantum processing by QuANNs, with implications for financial modeling. Indeed, while, traditionally, in financial econometrics one can see the distinction between a stochastic process (be it linear or nonlinear) and a deterministic nonlinear dynamical system, in the case of QuANNs applied to financial modeling they synthesize both approaches (stochastic and deterministic nonlinear), since the quantum state transition equations have a corresponding expression in a nonlinear deterministic dynamical system for probability measures assigned to the QuANN's statistical description via the correspondence between the projection norm dynamics and the statistical expectation associated to the projection operator.

The QuANNs application to financial modeling, thus, allows us to address the problem of simulating the resulting system dynamics that comes from a human cognition where interference patterns are found in the probabilistic description of human behavior.

2.3 A QUANTUM MARKET MODEL

Considering the financial case, a quantum regime switching model for the N volatility components plus the market polarization component, introduced in subsection 2.1, can be addressed through a Quantum Neural Automaton (QNA), defined as a one dimensional lattice with a QuANN associated to each lattice site, in this case we assume the lattice to have $N + 1$ sites and to each site k, for $k = 1,2 \ldots, N + 1$, is associated a QuANN with an architecture defined by a digraph with the following structure:

$$\Gamma = \left\{(n_1, n_2), (n_2, n_3), (n_3, n_1), (n_3, n_2)\right\} \qquad (39)$$

The corresponding Hilbert space for each such neural network $\mathrm{H}_{Net}(k)$ is $\mathrm{H}_2^{\otimes 3}$ that is $\mathrm{H}_{Net}(k) = \mathrm{H}_2^{\otimes 3}$, for $k = 1,2 \ldots, N + 1$, with the general basis vector $|s_1 s_2 s_3\rangle$, such that s_1 characterizes the activity pattern of the first neuron ($n_1(k)$), s_2 characterizes the second neuron ($n_2(k)$) and s_3 characterizes the activity pattern of the third neuron ($n_3(k)$).

In what follows, the neuron $n_3(k)$ encodes the market state for the corresponding component, $n_1(k)$ encodes the new market conditions supporting the corresponding component's dynamics and $n_2(k)$ addresses the computation of the synchronization pattern between $n_3(k)$ (the market state for the component) and $n_1(k)$ (the new market conditions).

The QNA Hilbert space $\mathrm{H}_{QNA} = \bigotimes_{k=1}^{N+1} \mathrm{H}_{Net}(k)$ is the tensor product of $N + 1$ copies of the Hilbert space $\mathrm{H}_2^{\otimes 3}$. Assuming this structure for the QNA, we now begin by addressing the local neural dynamics and its financial interpretation.

2.3.1 Local Neural Dynamics

Since the third neuron firing patterns encode the market state of the corresponding component, for the N volatility components, we have the neural network market volatility operator on $\mathrm{H}_2^{\otimes 3}$:

$$\hat{O}_V |s_1 s_2 0\rangle = v_0 |s_1 s_2 0\rangle \qquad (40)$$

$$\hat{O}_V |s_1 s_2 1\rangle = v_1 |s_1 s_2 1\rangle \qquad (41)$$

while for the market polarization component we have the neural network market polarization operator:

$$\hat{O}_P |s_1 s_2 0\rangle = -1 |s_1 s_2 0\rangle \qquad (42)$$

$$\hat{O}_P |s_1 s_2 1\rangle = +1 |s_1 s_2 1\rangle \qquad (43)$$

Since, as defined previously, $v_0 \leq v_1$, for a volatility neural network, when the third neuron fires we have a high volatility state, and when it does not fire we have a low volatility state. For the market polarization neural network, when the third neuron fires we have a *bullish* market state and when it does not fire we have a *bearish* market state.

Eqs. (40) to (43) show that both operators depend only on the third neuron's firing pattern, which means that, using Dirac's *bra-ket* notation, they can be expanded, respectively, as:

$$\begin{aligned} \hat{O}_V = {} & v_0 \left(\sum_{s_1, s_2 \in \mathrm{A}_2} |s_1 s_2 0\rangle\langle s_1 s_2 0| \right) + \\ & + v_1 \left(\sum_{s_1, s_2 \in \mathrm{A}_2} |s_1 s_2 1\rangle\langle s_1 s_2 1| \right) \end{aligned} \qquad (44)$$

$$\begin{aligned} \hat{O}_P = {} & -\left(\sum_{s_1, s_2 \in \mathrm{A}_2} |s_1 s_2 0\rangle\langle s_1 s_2 0| \right) + \\ & + \left(\sum_{s_1, s_2 \in \mathrm{A}_2} |s_1 s_2 1\rangle\langle s_1 s_2 1| \right) \end{aligned} \qquad (45)$$

Now, the neural network follows a closed loop starting at the market state neuron ($n_3(k)$) and ending at the market state neuron. The final state transition amplitudes and the underlying financial dynamics will depend upon the intermediate transformations which may change the profile of the corresponding component's state transition structure.

To address the neural dynamics and its relation with the financial market dynamics we need to introduce the neural links operators and follow the loop,

starting at $n_3(k)$ and ending at $n_3(k)$. Considering, then, the first neural link $n_3(k) \to n_1(k)$, we introduce the following neural network operator for the neuron $n_1(k)$:

$$\hat{L}_1 = \sum_{s\in\Lambda_2} e^{-\frac{i}{\hbar}\Delta t\hat{H}_0} \otimes |s\rangle\langle s| \otimes |0\rangle\langle 0| + \\ + \sum_{s'\in\Lambda_2} e^{-\frac{i}{\hbar}\Delta t\hat{H}_1} \otimes |s'\rangle\langle s'| \otimes |1\rangle\langle 1| \tag{46}$$

using Eq. (19) we need to define the angles $\theta(0)$, $\theta(1)$, $\omega(0)$, $\omega(1)$ and the unit vectors $\mathbf{u}(0)$, $\mathbf{u}(1)$, we set, in this case:

$$\frac{\theta(0)\Delta t}{2} = \varphi + \frac{\pi}{2}, \frac{\theta(1)\Delta t}{2} = \varphi \tag{47}$$

$$\frac{\omega(0)\Delta t}{2} = \pi, \frac{\omega(1)\Delta t}{2} = \frac{\pi}{2} \tag{48}$$

$$\mathbf{u}(0) = \mathbf{u}(1) = (1,0,0) \tag{49}$$

leading to the following operator structure:

$$e^{-\frac{i}{\hbar}\Delta t\hat{H}_0} = \sin(\varphi)\hat{1} + i\cos(\varphi)\hat{\sigma}_1 = \\ = \begin{pmatrix} \sin(\varphi) & i\cos(\varphi) \\ i\cos(\varphi) & \sin(\varphi) \end{pmatrix} \tag{50}$$

$$e^{-\frac{i}{\hbar}\Delta t\hat{H}_1} = i\cos(\varphi)\hat{1} + \sin(\varphi)\hat{\sigma}_1 = \\ = \begin{pmatrix} i\cos(\varphi) & \sin(\varphi) \\ \sin(\varphi) & i\cos(\varphi) \end{pmatrix} \tag{51}$$

the action of the operator $\hat{L}_1$ on the basis states is given by:

$$\hat{L}_1 |s_1 s_2 0\rangle = \sin(\varphi)|s_1 s_2 0\rangle + i\cos(\varphi)|1 - s_1 s_2 0\rangle \tag{52}$$

$$\hat{L}_1 |s_1 s_2 1\rangle = i\cos(\varphi)|s_1 s_2 1\rangle + \sin(\varphi)|1 - s_1 s_2 1\rangle \tag{53}$$

The operator $\hat{L}_1$ can be considered in terms of a quantum regime switching model, such that if the market state neuron $n_3(k)$ is not firing, then, $\sin(\varphi)$ is the amplitude associated to the alternative where the neuron $n_1(k)$ does not change state, while $i\cos(\varphi)$ is the amplitude associated to the alternative where the neuron $n_1(k)$ changes state, on the other hand, if the neuron $n_3(k)$ is firing the role of the amplitudes flip: $i\cos(\varphi)$ is associated with the alternative where the neuron $n_1(k)$ does not change state and $\sin(\varphi)$ is the amplitude associated with the alternative where the neuron $n_1(k)$ changes state.

Before considering the financial implications of this dynamics, it is necessary to address the rest of the network, because the final dynamics and its financial implications can only be fully addressed at the end of the cycle. As we will see, the end result will be a quantum computation-based selection process of adaptive rules regarding market expectations and the processing of how financial news may support trading decisions affecting market polarization and market volume.

Proceeding, then, with the neural links, the second neuron to be activated is $n_2(k)$, which, following the network architecture defined in Eq. (39) receives an input from the two neurons $n_1(k)$ and $n_3(k)$, this neuron will play a key role in the selection of adaptive rules regarding the relation between trading profiles and financial news, a point that we will return to when the final neural network state transition is analyzed. Following the quantum circuit framework, the second neuron is transformed conditionally on the states of the two neurons $n_1(k)$ and $n_3(k)$, in accordance with the neural links $n_1(k) \to n_2(k) \leftarrow n_3(k)$, the corresponding neural links operator is given by:

$$\hat{L}_2 = \sum_{s,s'\in\Lambda_2} |s\rangle\langle s| \otimes e^{-\frac{i}{\hbar}\Delta t\hat{H}_{ss'}} \otimes |s'\rangle\langle s'| \tag{54}$$

When the input neurons have synchronized firing patterns, the rotation and phase transformation angles are set to:

$$\frac{\theta(00)\Delta t}{2} = \frac{\theta(11)\Delta t}{2} = 0 \tag{55}$$

$$\frac{\omega(00)\Delta t}{2} = \frac{\omega(11)\Delta t}{2} = 0 \tag{56}$$

which means that the operators reduce to:

$$e^{-\frac{i}{\hbar}\Delta t\hat{H}_{00}} = e^{-\frac{i}{\hbar}\Delta t\hat{H}_{11}} = \hat{1} \tag{57}$$

that is, the second neuron remains in the same state when the input neurons ($n_1(k)$ and $n_3(k)$) exhibit a synchronized firing pattern (no rotation nor phase transformation takes place). When the input neurons do not exhibit a synchronized firing pattern, the rotation and phase transformation is set by the following parameters:

$$\frac{\theta(01)\Delta t}{2} = \frac{\theta(10)\Delta t}{2} = \frac{\pi}{2} \tag{58}$$

$$\frac{\omega(01)\Delta t}{2}=\frac{\omega(10)\Delta t}{2}=\frac{\pi}{2} \tag{59}$$

$$\mathbf{u}(01)=\mathbf{u}(10)=(1,0,0) \tag{60}$$

which leads to:

$$e^{-\frac{i}{\hbar}\Delta t\hat{H}_{01}}=e^{-\frac{i}{\hbar}\Delta t\hat{H}_{10}}=\hat{\sigma}_1 \tag{61}$$

thus, the action of $\hat{L}_2$ on each basis state is such that:

$$\hat{L}_2\left|ss_2s\right\rangle=\left|ss_2s\right\rangle \tag{62}$$

$$\hat{L}_2\left|ss_21-s\right\rangle=\left|s1-s_21-s\right\rangle \tag{63}$$

that is, the neuron $n_2(k)$ does not change state when the two neurons $n_1(k)$ and $n_3(k)$ have the same firing pattern, and flips state when the two neurons have differing firing patterns (this is equivalent to a controlled negation quantum circuit).

Now, to close the cycle, and before addressing the final dynamics and its financial interpretation, we have to address, first, the third link $n_2(k)\rightarrow n_3(k)$. In this case, we also introduce a controlled-negation circuit, so that the corresponding operator is:

$$\hat{L}_3=\sum_{s\in\Lambda_2}\left|s\right\rangle\left\langle s\right|\otimes\left|0\right\rangle\left\langle 0\right|\otimes e^{-\frac{i}{\hbar}\Delta t\hat{H}_0}+ \\ +\sum_{s'\in\Lambda_2}\left|s'\right\rangle\left\langle s'\right|\otimes\left|1\right\rangle\left\langle 1\right|\otimes e^{-\frac{i}{\hbar}\Delta t\hat{H}_1} \tag{64}$$

$$\frac{\theta(0)\Delta t}{2}=0,\frac{\theta(1)\Delta t}{2}=\frac{\pi}{2} \tag{65}$$

$$\frac{\omega(0)\Delta t}{2}=0,\frac{\omega(1)\Delta t}{2}=\frac{\pi}{2} \tag{66}$$

$$\mathbf{u}(1)=(1,0,0) \tag{67}$$

leading to:

$$e^{-\frac{i}{\hbar}\Delta t\hat{H}_0}=\hat{1},e^{-\frac{i}{\hbar}\Delta t\hat{H}_1}=\hat{\sigma}_1 \tag{68}$$

so that the basis states transform as:

$$\hat{L}_3\left|s_10s_3\right\rangle=\left|s_10s_3\right\rangle \tag{69}$$

$$\hat{L}_3\left|s_11s_3\right\rangle=\left|s_11-s_3\right\rangle \tag{70}$$

these equations show that the neuron $n_3(k)$ changes state when the second neuron is firing and does not change state when the second neuron is not firing. The neural network operator $\hat{L}_{Net}$ is the product of the three operators, that is:

$$\hat{L}_{Net}=\hat{L}_3\hat{L}_2\hat{L}_1 \tag{71}$$

Table 1 (in appendix) shows the results of the action of the neural network operator on each basis state.

From a financial perspective, table 1 synthesizes two adaptive rules, one in which the new market state for the component follows the new market conditions underlying the corresponding component's dynamics (neurons' $n_1(k)$ and $n_3(k)$ show a neural reinforcement dynamics), and another in which the new market state is contrarian with respect to the new market conditions underlying the corresponding component's dynamics (neurons' $n_1(k)$ and $n_3(k)$ show a neural inhibitory dynamics). These are two basic rules regarding expectation formation from new data: the decision to follow the new data or not.

In the first case, and taking as example a volatility component, the market is driven by an expectation of continuance of market conditions, so that, for instance, if market conditions are favorable to a high volatility state (neuron $n_1(k)$ is firing), then, the new market state follows the market conditions and $n_3(k)$ fires, corresponding to high volatility.

On the other hand, still under the first adaptive rule, if market conditions are unfavorable to a high volatility state (neuron $n_1(k)$ is not firing), then, the new market state follows the market conditions and $n_3(k)$ does not fire, corresponding to low volatility.

The resulting adaptive rule corresponds, thus, to a *follow the news* rule. Likewise, if we consider, instead, the market polarization component, the *follow the news* rule means that if the new market conditions support a bullish market sentiment, then, the market becomes bullish and if the new market conditions support a bearish market sentiment, then, the market becomes bearish.

The second adaptive rule is the reverse, expectations are that the new market conditions will not hold, and the market does the opposite from the news, expecting speculative gains.

The first adaptive rule is implemented when the second neuron is not firing, while the second rule is implemented when the second neuron is firing. Thus, the firing of the second neuron is a dynamical component that simulates a market change in its expectation and trading profile, so that, for the neural configurations $\{|000\rangle,|001\rangle,|100\rangle,|101\rangle\}$, the state transition for the market component's dynamics is driven by the first adaptive rule, while, for the neural configurations $\{|010\rangle,|011\rangle,|110\rangle,|111\rangle\}$, the market component's dynamics is driven by the second adaptive rule.

While neuron $n_2(k)$'s firing pattern determines the selection of a *follow the news rule*, the combination of firing patterns of the three neurons determines the quantum amplitudes for the market state transitions. Thus, when the neuron $n_2(k)$ is not firing, if the initial market conditions are aligned with the initial market state, then: sin(φ) is the amplitude associated with the alternative in which $n_1(k)$ and $n_3(k)$ transition to a not firing state and $i$cos(φ) is the amplitude associated with the alternative in which $n_1(k)$ and $n_3(k)$ transition to a firing state.

For a market volatility component, this means that a transition to a high volatility state, supported by market conditions, has an associated quantum amplitude of $i$cos(φ), while a market transition to a low volatility, state supported by market conditions, has an associated amplitude of sin(φ). The role of these amplitudes switches when $n_1(k)$ and $n_3(k)$ are not initially aligned.

When the neuron $n_2(k)$ is firing, the transition amplitudes to firing/non-firing states follow the same pattern as above for neuron $n_1(k)$ but reverse the pattern for neuron $n_3(k)$ because the new market conditions' neuron and the market state neuron transition to a non-aligned state (the market is contrarian with respect to the news), so that, if $n_1(k)$ and $n_3(k)$ are initially aligned, sin(φ) is the amplitude associated with a transition to the state where $n_1(k)$ is not firing and $n_3(k)$ is firing, while, if $n_1(k)$ and $n_3(k)$ are not initially aligned, the amplitude associated with such a transition is $i$cos(φ). The roles of the amplitudes, thus, depend upon the way in which the market adapts to new information and the previous configuration of market conditions and market state.

As expected, the market conditions and the market state neurons are always entangled, which means that, in each case, the market state effectively becomes like a measurement apparatus of the market conditions, the entanglement profile can, however, be aligned (*follow the news rule*, based on an expectation of sustainability of the new market conditions) or non-aligned (*contrarian rule*, based on the expectation of reversal of the new market conditions).

Thus, in the model, the quantum neural dynamics models a market that processes the information on the market conditions implementing a standard quantum measurement, but the profile of that quantum measurement depends upon the expectations regarding the news (leading to different entanglement profiles).

The final dynamics for the market component results from the iterative application of the operator $\hat{L}_{Net}$ for each trading round, leading to state transitions between the adaptive rules and, thus, between the market states. Considering a sequence of neural states for the market component's associated neural network $|\psi(k,t)\rangle$, the state transition resulting from the dynamical rule is given by:

$$|\psi(k,t)\rangle = \hat{L}_{Net}|\psi(k,t-\Delta t)\rangle \tag{72}$$

which leads to the following update rule for the quantum amplitudes ψ_k (as per the general Eq. (33)):

$$\begin{aligned}\psi_k(\mathbf{s},t) &= \sum_{\mathbf{s}'\in A_2^3}\langle \mathbf{s}|\hat{L}_{Net}|\mathbf{s}'\rangle\langle \mathbf{s}'\,|\,\psi(k,t-\Delta t)\rangle = \\ &= \sum_{\mathbf{s}'\in A_2^3} L_{Net}(\mathbf{s},\mathbf{s}')\psi_k(\mathbf{s}',t-\Delta t)\end{aligned} \tag{73}$$

using Table 1's results, in conjunction with this last equation, we obtain the transition table for the quantum amplitudes shown in table 2, provided in the appendix.

Taking into account this general neural dynamics for each component we can now piece it all together to address the market state and resulting financial dynamics.

2.3.2 Financial Market Dynamics

To address the full market dynamics we need to recover the QNA. For each trading round, the quantum state associated with the market dynamics is given by the QNA state defined as the tensor product of the lattice sites' neural networks' states, that is, by the tensor product of each component's neural network state:

$$\begin{aligned}|\psi(t)\rangle &= \bigotimes_{k=1}^{N+1}|\psi(k,t)\rangle = \\ &= \Psi(\mathbf{s}_1,\mathbf{s}_2,\ldots,\mathbf{s}_{N+1},t)|\mathbf{s}_1,\mathbf{s}_2,\ldots,\mathbf{s}_{N+1}\rangle\end{aligned} \tag{74}$$

where the quantum amplitudes $\Psi(s_1, s_2, \ldots, s_{N+1}, t)$ are given by:

$$\Psi(\mathbf{s}_1,\mathbf{s}_2,\ldots,\mathbf{s}_{N+1},t) = \prod_{k=1}^{N+1}\psi_k(\mathbf{s}_k,t) \tag{75}$$

with ψ_k being the amplitudes associated with the lattice site k's neural network.

For the N volatility components we can introduce a corresponding volatility operator on the QNA Hilbert space:

$$\hat{O}_k = \hat{1}^{\otimes k-1}\otimes\hat{O}_V\otimes\hat{1}^{\otimes N+1-k} \tag{76}$$

with $k = 1, \ldots, N$, where, as before, $\hat{1}^{\otimes m}$ denotes m-tensor product of the unit operator on H_2 and $\hat{O}_V$ is the volatility operator defined in Eqs. (40) and (41). Similarly, for the market polarization operator, we write:

$$\hat{O}_{N+1} = \hat{1}^{\otimes N} \otimes \hat{O}_P \tag{77}$$

where $\hat{O}_P$ is the market polarization operator defined in Eqs. (42) and (43). In this way, the returns' dynamical variable defined in Eq. (8) is replaced, in the quantum econophysics setting, by a quantum operator on the QNA Hilbert space defined as:

$$\hat{R} = \frac{1}{\lambda}\prod_{k=1}^{N+1}\hat{O}_k \tag{78}$$

For each basis state of the QNA Hilbert space, the returns operator has an eigenvalue given by the corresponding financial market returns:

$$\begin{aligned}\hat{R}\left|\mathbf{s}_1,\mathbf{s}_2,...,\mathbf{s}_{N+1}\right\rangle = \\ = R(\mathbf{s}_1,\mathbf{s}_2,...,\mathbf{s}_{N+1})\left|\mathbf{s}_1,\mathbf{s}_2,...,\mathbf{s}_{N+1}\right\rangle\end{aligned} \tag{79}$$

with the eigenvalues $R(\mathbf{s}_1, \mathbf{s}_2, ..., \mathbf{s}_{N+1})$ given by:

$$R(\mathbf{s}_1,\mathbf{s}_2,...,\mathbf{s}_{N+1}) = \frac{1}{\lambda}\prod_{k=1}^{N} v_k(\mathbf{s}_k)\cdot\sigma_{N+1}(\mathbf{s}_{N+1}) \tag{80}$$

where $v_k(\mathbf{s}_k) = v_0$ if the binary string $\mathbf{s}_k \in \mathrm{A}_2^3$ ends in 0 ($n_3(k)$ is not firing) and $v_k(\mathbf{s}_k) = v_1$ if the binary string $\mathbf{s}_k$ ends in 1 ($n_3(k)$ is firing), similarly $\sigma_{N+1}(\mathbf{s}_{N+1}) = -1$ if $\mathbf{s}_{N+1} \in \mathrm{A}_2^3$ ends in 0 ($n_3(N+1)$ is not firing) and ($\sigma_{N+1}(\mathbf{s}_{N+1}) = 1$ if $\mathbf{s}_{N+1}$ ends in 1 ($n_3(N+1)$ is firing).

The dynamical rule that comes from the neural networks' quantum computation leads to the market state transition for each trading round:

$$\left|\psi(t)\right\rangle = \bigotimes_{k=1}^{N+1}\hat{L}_{Net}\left|\psi(k,t-\Delta t)\right\rangle \tag{81}$$

leading to the expected value for the returns:

$$\begin{aligned}\left\langle\hat{R}\right\rangle_t = \\ = \sum_{\mathbf{s}_1,\mathbf{s}_2,...,\mathbf{s}_{N+1}} R(\mathbf{s}_1,\mathbf{s}_2,...,\mathbf{s}_{N+1})\left|\Psi(\mathbf{s}_1,\mathbf{s}_2,...,\mathbf{s}_{N+1},t)\right|^2\end{aligned} \tag{82}$$

so that the market tends to the alternative $R(\mathbf{s}_1, \mathbf{s}_2, ..., \mathbf{s}_{N+1})$ with an associated probability of $\left|\Psi(\mathbf{s}_1,\mathbf{s}_2,...,\mathbf{s}_{N+1},t)\right|^2$.

The following figure shows a market simulation on Python 3.4. In the simulations, the initial state for each component is taken from a randomly chosen $U(2)$ gate applied to each neuron with uniform probability over $U(2)$. The figure shows the markers of financial turbulence in the returns, including volatility bursts and jumps.

The main parameters that determine the market profile with regards to turbulence is v_0 and the number of components, the turbulence profile does not change much with respect to the rotation angle φ. Indeed, as shown in the table 3, provided in the appendix, the estimated kurtosis[10] for different simulations with 20 components tends to decrease as v_0 rises. For $v_0 = 0.9$ we no longer find excess kurtosis, the turbulence markers being lost. This approach to low turbulence is progressive as v_0 is raised from 0.8 to 0.9, such that that the price jumps tend to become less severe and less frequent, and the volatility bursts tend to disappear, as shown in Figure 2, in which $v_0 = 0.9$ with the rest of the parameters used in Figure 1's simulation being left unchanged.

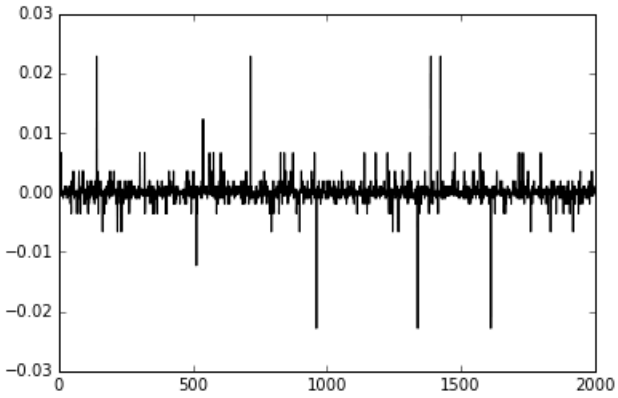

Figure 1. Simulation of the financial returns for $\sin^2\varphi = 0.6$, $v_0 = 0.7$, $\lambda = 1000$, 20 components (19 volatility components plus 1 polarization component). The figure shows 2000 data points of a 2100 data points simulation with the first 100 points removed for transients.

The model, thus, captures different market profiles: as the parameter v_0 increases from 0.8 to 0.9 the simulations tend to approach a lower tail risk dynamics, with a greater approximation to the classical Gaussian returns' probability model occurring for v_0 near 0.87, the table 4 in appendix shows this approximation with the kurtosis values and Jarque-Bera test for normality, as the value of v_0 is increased.

As shown in table 4, for every value of v_0 the Jarque-Bera's null hypothesis is rejected at 1% significance level except for $v_0 = 0.87$. It is important to stress however, that although simulated returns distribution can approximate the Gaussian distribution, this approximation is not robust, different simulations for the same parameters may show deviations from the Gaussian distribution.

Table 5, in appendix, shows examples of simulations for different values of the rotation angle φ, with $v_0 = 0.87$, the null hypothesis of Jarque-Bera's test is not reject, at a 1% significance, for $\sin^2\varphi = 0.1, 0.3, 0.6$, with $\sin^2\varphi = 0.1, 0.3$ as the only cases in which it is not rejected for 5% significance, and $\sin^2\varphi = 0.3$ as

[10] The Fisher kurtosis is used in the statistical analysis of the model's outputs.

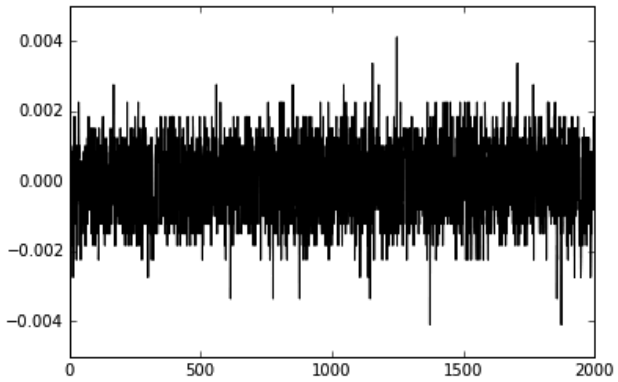

Figure 2. Simulation of financial returns for $\sin^2\varphi = 0.6$, $v_0 = 0.9$, $\lambda = 1000$, 20 components (19 volatility components plus 1 polarization component). The figure shows 2000 data points of a 2100 data points simulation with the first 100 points removed for transients.

the only case in which it is not rejected also for a 10% significance.

These results may, however, depend, as stated previously, upon the simulation, other simulations may show the null hypothesis being rejected for the same parameters, which means that the Gaussian distribution depends upon the sample path and is not a dynamically fixed probability law that can be assumed to hold indefinitely.

The general tail risk pattern, on the other hand, is more robust than the Gaussian approximation, in the sense that as v_0 approaches 0.9 and for $v_0 \geq 0.9$, the market loses the turbulence profile with the jumps and volatility changes becoming less frequent and the kurtosis becoming less and less leptokurtic, leading to lower tail risk, the market returns eventually fluctuate randomly around a narrow band.

Underlying the complex behavior of the simulated market returns is the probability dynamics that comes from the neural network's iterative scheme shown in table 2. Considering Eqs. (35) to (37) and combining with table 2's results we get, in this case, sixteen nonlinear dynamical equations of the general form:

$$A_k(\mathbf{s},t) = \left[\begin{array}{l}\sqrt{A_k(\mathbf{s}',t-\Delta t)}\sin(\varphi) - \\ \sqrt{B_k(\mathbf{s}'',t-\Delta t)}\cos(\varphi)\end{array}\right]^2 \tag{83}$$

$$B_k(\mathbf{s},t) = \left[\begin{array}{l}\sqrt{B_k(\mathbf{s}',t-\Delta t)}\sin(\varphi) + \\ \sqrt{A_k(\mathbf{s}'',t-\Delta t)}\cos(\varphi)\end{array}\right]^2 \tag{84}$$

with $\mathbf{s},\mathbf{s}',\mathbf{s}'' \in \mathrm{A}_2^3$ and $\mathbf{s}' \neq \mathbf{s}''$, so that the probability dynamics that come from the neural network's evolution can be addressed by a nonlinear map with sixteen dynamical variables satisfying the normalization rule:

$$\sum_{\mathbf{s}} A_k(\mathbf{s},t) + \sum_{\mathbf{s}'} B_k(\mathbf{s}',t) = 1 \tag{85}$$

with the probability of the neural configuration **s** being given by the sum:

$$Prob_k[\mathbf{s},t] = A_k(\mathbf{s},t) + B_k(\mathbf{s},t) \tag{86}$$

so that the probability distribution for the neural configurations is a function of a sixteen dimensional nonlinear map on a hypersphere of unit radius (due to the normalization condition).

If we expand the squares in Eqs. (83) and (84) we get:

$$\begin{aligned} A_k(\mathbf{s},t) = {} & A_k(\mathbf{s}',t-\Delta t)\sin^2(\varphi) + \\ & + B_k(\mathbf{s}'',t-\Delta t)\cos^2(\varphi) - \\ & - \sqrt{A_k(\mathbf{s}',t-\Delta t)B_k(\mathbf{s}'',t-\Delta t)}\sin(2\varphi) \end{aligned} \tag{87}$$

$$\begin{aligned} B_k(\mathbf{s},t) = {} & B_k(\mathbf{s}',t-\Delta t)\sin^2(\varphi) + \\ & + A_k(\mathbf{s}'',t-\Delta t)\cos^2(\varphi) + \\ & + \sqrt{B_k(\mathbf{s}',t-\Delta t)A_k(\mathbf{s}'',t-\Delta t)}\sin(2\varphi) \end{aligned} \tag{88}$$

which leads to the following expansion for the probability:

$$\begin{aligned} Prob_k[\mathbf{s},t] = {} & Prob_k[\mathbf{s}',t-\Delta t]\sin^2(\varphi) + \\ & + Prob_k[\mathbf{s}'',t-\Delta t]\cos^2(\varphi) + \\ & + \sqrt{B_k(\mathbf{s}',t-\Delta t)A_k(\mathbf{s}'',t-\Delta t)}\sin(2\varphi) - \\ & - \sqrt{A_k(\mathbf{s}',t-\Delta t)B_k(\mathbf{s}'',t-\Delta t)}\sin(2\varphi) \end{aligned} \tag{89}$$

the quantum interference terms (that correspond to the square root terms multiplied by $\sin(2\varphi)$ in Eq. (89)) have an expression, at the probability level, that can be approached in terms of a classical nonlinear dynamical system for the probabilities.

In the classical nonlinear dynamics representation, each financial returns component's stochastic dynamics has a probability measure that updates at each trading round with a deterministic nonlinear update rule, this establishes the bridge between the stochastic process and the nonlinear deterministic dynamical systems modeling of financial dynamics: the neural network's quantum dynamics leads to a nonlinear deterministic dynamics in the probabilities.

A question that may be raised regards the transition from the deterministic nonlinear map to a noisy nonlinear map, from the financial perspective this makes sense since external stochastic factors may affect the financial system. A possible solution for this might be to allow the rotation angle φ to change, so

that instead of a fixed value of φ we replace it by a random variable $\varphi_k(t)$ in Eqs. (83) and (84) so that we get a stochastic nonlinear dynamical system. The introduction of a random $\varphi_k(t)$ implies that we are no longer dealing with a fixed unitary operator structure for the QuANN but, instead, work with a quantum neural state transition with a random component in the Hamiltonian, that is, the unitary gates of Eqs. (50) and (51) are now stochastic unitary gates:

$$e^{-\frac{i}{\hbar}\Delta t\hat{H}_0(t)} = \begin{pmatrix} \sin\left(\varphi_k(t)\right) & i\cos\left(\varphi_k(t)\right) \\ i\cos\left(\varphi_k(t)\right) & \sin\left(\varphi_k(t)\right) \end{pmatrix} \quad (90)$$

$$e^{-\frac{i}{\hbar}\Delta t\hat{H}_1(t)} = \begin{pmatrix} i\cos\left(\varphi_k(t)\right) & \sin\left(\varphi_k(t)\right) \\ \sin\left(\varphi_k(t)\right) & i\cos\left(\varphi_k(t)\right) \end{pmatrix} \quad (91)$$

Thus, a stochastic nonlinear map is induced by the quantum noisy gates in the QuANN's state transition rule, coming from a stochastic Hamiltonian. Figure 3, below, shows the simulation results for:

$$\varphi_k(t) = \arcsin\left(\frac{1}{\sqrt{1+e^{-2\beta z_k(t)}}}\right) \quad (92)$$

with $z_k(t) \sim N(0,1)$, which leads to:

$$\sin^2\left(\varphi_k(t)\right) = \frac{1}{1+e^{-2\beta z_k(t)}} \quad (93)$$

$$\cos^2\left(\varphi_k(t)\right) = \frac{e^{-2\beta z_k(t)}}{1+e^{-2\beta z_k(t)}} \quad (94)$$

the logistic function present in Eqs. (93) and (94) is also widely used in classical ANNs for the activation probability and leaves room for expansion of connections to Statistical Mechanics (Müller and Strickland, 1995). If we replace in Eq. (89) we get the nonlinear stochastic equations for the probabilities:

$$\begin{aligned} Prob_k[\mathbf{s},t] &= \frac{Prob_k[\mathbf{s}',t-\Delta t]}{1+e^{-2\beta z_k(t)}} \\ &+ \frac{Prob_k[\mathbf{s}'',t-\Delta t]e^{-2\beta z_k(t)}}{1+e^{-2\beta z_k(t)}} + \\ &+ 2\sqrt{B_k(\mathbf{s}',t-\Delta t)A_k(\mathbf{s}'',t-\Delta t)}\frac{e^{-\beta z_k(t)}}{1+e^{-2\beta z_k(t)}} - \\ &- 2\sqrt{A_k(\mathbf{s}',t-\Delta t)B_k(\mathbf{s}'',t-\Delta t)}\frac{e^{-\beta z_k(t)}}{1+e^{-2\beta z_k(t)}} \end{aligned} \quad (95)$$

Figure 3 shows the occurrence of price jumps and clustering volatility, the turbulence in this case is linked to the high number of components (rather than to the noisy gates). Indeed, as tables 6. and 7., provided in the appendix, show, the noisy gates do not have a strong effect on the transition from leptokurtic to platikurtic distributions, both for low and high values of β, it is the number of components that has a stronger impact on market profile, as seen in table 7 for the case of $v_0 = 0.88$ which for the simulation with $\beta = 2$ was close enough to the Gaussian distribution for the non-rejection of the null hypothesis of the Jarque-Bera test at a 10% significance level.

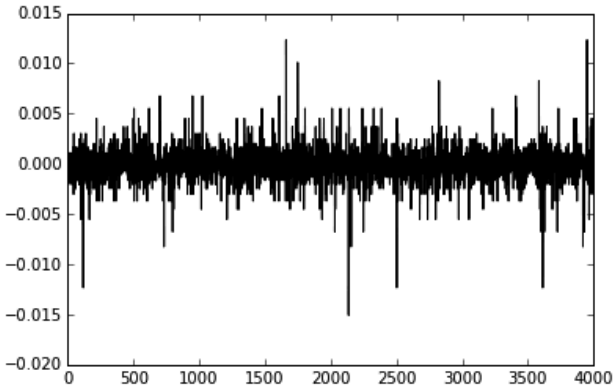

Figure 3. Simulation of financial returns for noisy gates with $\beta = 2.0$, $v_0 = 0.9$, $\lambda = 1000$, 80 components (79 volatility components plus 1 polarization component). The figure shows 4000 data points of a 4100 data points simulation with the first 100 points removed for transients.

Indeed, the number of components shows a strong effect, as can be seen in figure 3, which uses $v_0 = 0.9$ and in table 7, that shows the transition from platikurtic to leptokurtic for large values of the components, for both a low and a high value of β.

3. FINANCE, NONLINEAR STOCHASTIC DYNAMICS AND QUANTUM ARTIFICIAL INTELLIGENCE

From the early onset of development of econophysics, some form of nonlinear stochastic dynamics has been considered to be present in financial market dynamics. A major example being Vaga's work that addressed explicitly different probability distributions corresponding to different (classical) Hamiltonian conditions (Vaga, 1990). The major point that markets make transitions between different regimes and different probability distributions was key to Vaga's market theory. On the other hand, the multifractal multiplicative cascades (Mandelbrot *et al.*, 1997) introduced multiplicative stochastic processes as sources of market turbulence.

While a division line is drawn in regards to nonlinear deterministic processes versus nonlinear sto-

chastic processes, the possible combination of both might provide an intermediate approach, combining adaptive market dynamics and stochastic factors affecting market behavior.

As the previous section model shows, when recurrent QuANNs are applied to financial modeling, the nonlinear deterministic dynamics and the nonlinear stochastic processes result directly from the quantum computational structure, in the sense that: while the iterative computation of a QuANN results from the linear conditional unitary state transition, the corresponding probabilities, due to the square modulus rule for addressing the probabilities associated to different neural firing patterns, leads to a nonlinear update rule for the probabilities themselves, which means that the market behavior will show an interference effect at the probability level expressible in terms of a classical nonlinear map, thus, while the system follows a stochastic dynamics, the probabilities are updated nonlinearly.

This is a direct consequence of quantum cognitive science that comes from human decision analysis, which shows that the nonlinear update in probabilities, leading to non-additive decision weights may be computationally approached from linear unitary quantum computation on an appropriate Hilbert space. Stochastic factors in the nonlinear update of probabilities can also be introduced through unitary noise in the neural network's computation through stochastic Hamiltonians.

Although QuAI and QuANN theory are still on their early stages, they provide a bridge between major lines of research on financial dynamics and risk modeling including: nonlinear deterministic and stochastic dynamics applied to financial modeling, cognitive science and computational foundations of financial theory. Future research on QuANNs dynamics may thus serve as a relevant tool to link different approaches that characterized the different lines of research on econophysics-based finance.

REFERENCES

Anderson, P.W., Arrow, K.J. & Pines, D. (eds.) (1988), *The Economy as an Evolving Complex System*, Perseus Books, USA.

Arthur, B.W., Durlauf, S.N. & Lane, D. (eds.) (1997), *The Economy as an Evolving Complex System II*, Westview Press, USA.

Baaquie, B.E., Kwek, L.C. & Srikant, M. (2000), "Simulation of Stochastic Volatility using Path Integration: Smiles and Frowns", www. arXiv. org.

Baaquie, B.E. & Marakani, S. (2001), "Empirical investigation of a quantum field theory of forward rates", www. arXiv. org.

Baaquie, B.E. (2004), *Quantum Finance: Path Integrals and Hamiltonians for Options and Interest Rates*, Cambridge University Press, USA.

Baaquie, B.E. & Pan, T. (2011), "Simulation of coupon bond European and barrier options in quantum finance", Physica A, 390, 263–289.

Behrman, E.C., Niemel, J., Steck, J.E. & Skinner, S.R. (1996), "A Quantum Dot Neural Network", in Toffoli, T. and Biafore, M. (eds), *Proceedings of the 4th Workshop on Physics of Computation*, Elsevier Science Publishers, Amsterdam, 22–24.

Bohm, D. (1984), *Causality and Chance in Modern Physics*, (1997 Reprinted Version) Routledge & Kegan Paul, Eastbourne.

Bohm, D. & Hiley, B.J. (1993), *The undivided universe — An ontological interpretation of quantum theory*, Routledge, London.

Bransden, B.H. & Joachain, C.J. (2000), *Quantum Mechanics*, Prentice Hall, England.

Bruce, C. (2004), *Schrödinger's Rabbits — the many worlds of quantum*, Joseph Henry Press, Washington DC.

Brunn, C. (ed.) (2006), *Advances in Artificial Economics — The Economy as a Complex Dynamic System*, Springer, Berlin.

Busemeyer, J.R. & Franco, R. (2010), "What is The Evidence for Quantum Like Interference Effects in Human Judgments and Decision Behavior?", NeuroQuantology, vol. 8, No. 4: S48–62.

Busemeyer, J.R. & Bruza, P.D. (2012), *Quantum models of cognition and decision*, Cambridge University Press, Cambridge.

Busemeyer, J.R. & Wang, Z. (2014), "Quantum Cognition: Key Issues and Discussion", Topics in Cognitive Science 6: 43–46.

Calvet, L. & Fisher, A. (2002), "Multifractality in asset returns: Theory and evidence", Review of Economics and Statistics, Vol. 84, 3, August, 381–406.

Calvet, L. & Fisher, A. (2004), "Regime-switching and the estimation of multifractal processes", Journal of Financial Econometrics, 2: 44–83.

Choustova, O. (2007a), "Quantum modeling of nonlinear dynamics of stock prices: Bohmian approach", Theoretical and Mathematical Physics, 152 (2): 1213–1222.

Choustova, O. (2007b), "Toward quantum-like modeling of financial processes", J.Phys.: Conf. Ser. 7001 2006.

Chrisley, R. (1995), "Quantum learning", in Pylkkänen, P. & Pylkkö, P. (eds.), *New directions in cognitive science: Proceedings of the international symposium*, Saariselka, 4–9 August, Lapland, Finland, Finnish Artificial Intelligence Society, Helsinki, 77–89.

Deutsch, D. (1985), "Quantum theory, the Church-Turing Principle and the universal quantum computer", Proc R Soc Lond A, 400–497.

Deutsch, D. (1999), "Quantum theory of probability and decisions", Proc.R.Soc. Lond. A 1999 455 3129–3137.

DeWitt, B.S. (1970), "Quantum mechanics and reality — Could the solution to the dilemma of indeterminism be a universe in which all possible outcomes of an experiment actually occur?", Physics Today, Vol. 23, No. 9, 155–165.

Dirac, P.A.M. (1967), *The Principles of Quantum Mechanics (Fourth Edition)*, Claredon Press, Oxford.

Everett, H. (1957), "'Relative state' formulation of quantum mechanics", Rev. of Mod. Physics, 29 (3): 454–462.

Everett, H. (1973), "The Theory of the Universal Wavefunction, PhD Manuscript", in DeWitt, R. & Graham, N. (eds.), *The*

Many-Worlds Interpretation of Quantum Mechanics, Princeton Series in Physics, Princeton University Press, 3–140.

Ehrentreich, N. (2008), *Agent-Based Modeling — The Santa Fe Institute Artificial Stock Market Model Revisited*, Springer, Berlin.

Farmer, D. (2002), "Market force, ecology and evolution", Industrial and Corporate Change, 11 (5): 895–953.

Focardi, S.M. & Fabozzi, F.J. (2004), *The Mathematics of Financial Modeling and Investment Management*, John Wiley and Sons, New Jersey.

Gonçalves, C.P. (2011), "Financial turbulence, business cycles and intrinsic time in an artificial economy", Algorithmic Finance, 1 (2): 141–156.

Gonçalves, C.P. (2013), "Quantum Financial Economics — Risk and Returns", J Syst Sci Complex, 26: 187–200.

Gonçalves, C.P. (2015), "Quantum Cybernetics and Complex Quantum Systems Science — A Quantum Connectionist Exploration", NeuroQuantology, vol. 13, No. 1: 35–48.

Greiner, W, & Müller, B. (2001), *Quantum Mechanics Symmetries*, Springer, Germany.

Haven, E. & Khrennikov, A. (2013), *Quantum Social Science*, Cambridge University Press, New York.

Haken, H. (1977), *Synergetics: An Introduction*, Springer, Germany.

Iori, G. (1999), "Avalanche Dynamics and Trading Friction Effects on Stock Market Returns", Int.J.Mod. Phys. C, 10, 1149.

Ilinski, K. (2001), *Physics of Finance — Gauge Modelling in Non-equilibrium Pricing*, John Wiley and Sons, West Sussex.

Ivancevic, V.G. & Ivancevic T.T. (2010), *Quantum Neural Computation*, Springer, Dordrecht.

Kak, S. (1995), "Quantum Neural Computing", Advances in Imaging and Electron Physics, vol. 94: 259–313.

Kauffman, S.A. (1993), *The Origins of Order — Self-Organization and Selection in Evolution*, Oxford University Press, New York.

Khrennikov, A. (2010), *Ubiquitous Quantum Structure: From Psychology to Finance*, Springer, Berlin.

Khrennikov, A. & Basieva, I. (2014), "Quantum Model for Psychological Measurements: From the Projection Postulate to Interference of Mental Observables Represented As Positive Operator Valued Measures", NeuroQuantology, vol. 12, No. 3: 324–336.

Leggett, A.J. (2002), "Qubits, Cbits, Decoherence, Quantum Measurement and Environment", in Heiss, D. (ed.), *Fundamentals of Quantum Information — Quantum Computation, Communication, Decoherence and All That*, Springer, Germany.

Lux, T. & Marchesi, M. (1999), "Scaling and criticality in a stochastic multi-agent model of a financial market", Nature 397, 498–500.

Lux, T. (2008), "The Markov-Switching Multifractal Model of Asset returns: GMM estimation and linear forecasting of volatility", Journal of Business and Economic Statistics, 26: 194–210.

Mandelbrot, B.B., Fisher, A. & Calvet, L. (1997), "A Multifractal Model of Asset Returns", Cowles Foundation Discussion Papers: 1164.

Mandelbrot, B.B. (1997), *Fractals and Scaling in Finance*, Springer, USA.

McCulloch, W. & Pitts, W. (1943), "A logical calculus of the ideas immanent in nervous activity", Bulletin of Mathematical Biophysics, 7: 115–133.

Menneer, T. & Narayanan, A. (1995), "Quantum-inspired Neural Networks", technical report R329, Department of Computer Science, University of Exeter, Exeter, United Kingdom.

Menneer T. (1998), *Quantum Artificial Neural Networks*, Ph. D. thesis, The University of Exeter, UK.

Müller, B., Reinhardt, J. & Strickland, M.T. (1995), *Neural Networks An Introduction*, Springer-Verlag, Berlin.

Nash, J. (1951), "Non-Cooperative Games", The Annals of Mathematics, Second Series, Vol. 54, No. 2, 286–295.

Nielsen, M. & Chuang, I. (2003), *Quantum Computation and Quantum Information*, The Press Syndicate of the University of Cambridge, UK.

Piotrowski, E.W. & Sładkowski, J. (2001), "Quantum-like approach to financial risk: quantum anthropic principle", Acta Phys. Polon., B32, 3873.

Piotrowski, E.W. & Sładkowski, J. (2002), "Quantum Market Games", Physica A, Vol. 312, 208–216.

Piotrowski, E.W. & Sładkowski, J. (2008), "Quantum auctions: Facts and myths", Physica A, Vol. 387, 15, 3949–3953.

Saptsin, V. & Soloviev, V. (2009), "Relativistic quantum econophysics — new paradigms in complex systems modelling", www. arXiv. org.

Saptsin, V. & Soloviev, V. (2011), "Heisenberg uncertainty principle and economic analogues of basic physical quantities", Computer Modelling and New Technologies, vol. 15, No. 3: 21–26.

Segal, W. & Segal, I.E. (1998), "The Black– Scholes pricing formula in the quantum context", PNAS March 31, vol. 95 no. 7, 4072–4075.

Vaga, T. (1990), "The Coherent Market Hypothesis", Financial Analysts Journal, 46, 6: 36–49.

Voit, J. (2001), *The Statistical Mechanics of Financial Markets*, Springer, New York.

Wallace, D. (2002), "Quantum Probability and Decision Theory, Revisited", www. arXiv. org.

Wallace, D. (2007), "Quantum Probability from Subjective Likelihood: improving on Deutsch's proof of the probability rule", Studies in the History and Philosophy of Modern Physics 38, 311–332.

Wang, Z. & Busemeyer, J.R. (2013), "A quantum question order model supported by empirical tests of an a priori and precise prediction", Topics in Cognitive Science, 5: 689–710.

Zuo, X. (2014), "Numerical Simulation of Asano-Khrennikov-Ohya Quantum-like Decision Making Model", NeuroQuantology, vol. 12, No. 4: 372–385.

APPENDIX – TABLES

Table 1. Neural network operator's action on the basis states.

Basis States	$\hat{L}_{Net}\|\mathbf{s}\rangle = \hat{L}_3\hat{L}_2\hat{L}_1\|\mathbf{s}\rangle$
$\|000\rangle$	$\sin(\varphi)\|000\rangle + i\cos(\varphi)\|111\rangle$
$\|001\rangle$	$i\cos(\varphi)\|010\rangle + \sin(\varphi)\|101\rangle$
$\|010\rangle$	$\sin(\varphi)\|011\rangle + i\cos(\varphi)\|100\rangle$
$\|011\rangle$	$i\cos(\varphi)\|001\rangle + \sin(\varphi)\|110\rangle$
$\|100\rangle$	$i\cos(\varphi)\|000\rangle + \sin(\varphi)\|111\rangle$
$\|101\rangle$	$\sin(\varphi)\|010\rangle + i\cos(\varphi)\|101\rangle$
$\|110\rangle$	$i\cos(\varphi)\|011\rangle + \sin(\varphi)\|100\rangle$
$\|111\rangle$	$\sin(\varphi)\|001\rangle + i\cos(\varphi)\|110\rangle$

Table 2. Update of the quantum amplitudes for a single market component.

New Amplitudes
$\psi_k(000,t) = \sin(\varphi)\psi_k(000,t-\Delta t) + i\cos(\varphi)\psi_k(100,t-\Delta t)$
$\psi_k(001,t) = i\cos(\varphi)\psi_k(011,t-\Delta t) + \sin(\varphi)\psi_k(111,t-\Delta t)$
$\psi_k(010,t) = i\cos(\varphi)\psi_k(001,t-\Delta t) + \sin(\varphi)\psi_k(101,t-\Delta t)$
$\psi_k(011,t) = \sin(\varphi)\psi_k(010,t-\Delta t) + i\cos(\varphi)\psi_k(110,t-\Delta t)$
$\psi_k(100,t) = i\cos(\varphi)\psi_k(010,t-\Delta t) + \sin(\varphi)\psi_k(110,t-\Delta t)$
$\psi_k(101,t) = \sin(\varphi)\psi_k(001,t-\Delta t) + i\cos(\varphi)\psi_k(101,t-\Delta t)$
$\psi_k(110,t) = \sin(\varphi)\psi_k(011,t-\Delta t) + i\cos(\varphi)\psi_k(111,t-\Delta t)$
$\psi_k(111,t) = i\cos(\varphi)\psi_k(000,t-\Delta t) + \sin(\varphi)\psi_k(100,t-\Delta t)$

Table 3. Kurtosis values for different values of $\sin^2\varphi$ and v_0. The other parameters are: $\lambda = 1000$, 20 components (19 volatility components plus 1 polarization component), the Kurtosis coefficient was calculated on 5000 sample data points of a 5100 data points simulation with the first 100 data points removed for transients.

	$\sin^2\varphi = 0.4$	$\sin^2\varphi = 0.5$	$\sin^2\varphi = 0.6$
$v_0 = 0.4$	585.4546	1336.6726	1923.3159
$v_0 = 0.5$	778.0387	1876.3810	783.0852
$v_0 = 0.6$	1015.5296	473.4505	383.9775
$v_0 = 0.7$	77.6054	49.5857	56.8335
$v_0 = 0.8$	6.8827	20.7037	5.6217
$v_0 = 0.9$	−0.8538	−1.2335	−0.9277

Table 4. Kurtosis values and Jarque-Bera test of normality for different values v_0. The other parameters are: $\sin^2\varphi = 0.6$, $\lambda = 1000$, 20 components (19 volatility components plus 1 polarization component), the Kurtosis coefficient was calculated on 5000 sample data points of a 5100 data points simulation with the first 100 data points removed for transients.

	Kurtosis	JB Statistic	p-value
$v_0 = 0.85$	1.2911	353.7757	0.0
$v_0 = 0.86$	0.3596	46.5669	7.7289e-11
$v_0 = 0.87$	0.1746	6.3179	0.0425
$v_0 = 0.88$	−0.0160	76.5797	0.0
$v_0 = 0.89$	−0.6790	106.5589	0.0
$v_0 = 0.9$	−0.8223	143.5983	0.0

Table 5. Kurtosis values for different values φ. The other parameters are: $v_0 = 0.87$, $\lambda = 1000$, 20 components (19 volatility components plus 1 polarization component), the Kurtosis coefficient was calculated on 5000 sample data points of a 5100 data points simulation with the first 100 data points removed for transients.

$\sin^2\varphi$	Kurtosis	JB Statistic	p-value
0.1	0.1285	4.8697	0.0876
0.2	0.6385	84.4538	0.0
0.3	0.0947	3.8794	0.1437
0.4	0.3169	35.1954	2.2773e-08
0.5	0.9213	565.5135	0.0
0.6	0.1746	6.3179	0.0425
0.7	0.0841	29.6076	3.7221e-07
0.8	0.4975	65.859	4.9960e-15
0.9	0.1775	31.3417	1.5640e-07

Table 6. Kurtosis values and Jarque-Bera test of normality p-values for different simulations with varying v_0 and noisy unitary gates. The other parameters are: $\beta = 0.01$ (left table) and $\beta = 2$ (right table), $\lambda = 100$, 20 components (19 volatility components plus 1 polarization component), the kurtosis coefficient was calculated on 5000 sample data points of a 5100 data points simulation with the first 100 data points removed for transients.

$\beta = 0.01$	Kurtosis	JB p-value	$\beta = 2$	Kurtosis	JB p-value
$v_0 = 0.86$	0.9171	0.0	$v_0 = 0.86$	0.7097	0.0
$v_0 = 0.87$	0.0345	1.0518e-07	$v_0 = 0.87$	0.1786	0.0018
$v_0 = 0.88$	−0.3647	2.8422e-13	$v_0 = 0.88$	−0.0856	0.3119
$v_0 = 0.89$	−0.7142	0.0	$v_0 = 0.89$	−0.6205	0.0
$v_0 = 0.9$	−0.6810	0.0	$v_0 = 0.9$	−0.8840	0.0

Table 7. Kurtosis values and Jarque-Bera test of normality for different values of the number of components (N +1) and noisy unitary gates. The other parameters are: $v_0 = 0.88$ $\beta = 0.01$ (left table) and $\beta = 2$ (right table), $\lambda = 100$, the kurtosis coefficient was calculated on 5000 sample data points of a 5100 data points simulation with the first 100 data points removed for transients.

$\beta = 0.01$	Kurtosis	p-value	$\beta = 2$	Kurtosis	p-value
N + 1 = 10	−1.3408	0.0	N + 1 = 10	−1.3752	0.0
N + 1 = 20	−0.3647	2.8422e-13	N + 1 = 20	−0.0856	0.3119
N + 1 = 30	1.6227	0.0	N + 1 = 30	2.2008	0.0
N + 1 = 40	2.5130	0.0	N + 1 = 40	3.4597	0.0
N + 1 = 50	10.1352	0.0	N + 1 = 50	15.9802	0.0